First-order design of off-axis reflective ophthalmic adaptive optics systems using afocal telescopes

Armando Gómez-Vieyra,[1] Alfredo Dubra,[2,*], Daniel Malacara-Hernández,[1]and David R. Williams[3]

[1]*Centro de Investigaciones en Óptica A.C., Loma del Bosque 115, C.P. 37000, León, Guanajuato, México*
[2] *University of Rochester Eye Institute, Rochester, NY, 14642-0314, USA*
[3]*Center for Visual Science, University of Rochester, Rochester, NY, 14627-0270, USA*
**adubra@cvs.rochester.edu*

Abstract: Expressions for minimal astigmatism in image and pupil planes in off-axis afocal reflective telescopes formed by pairs of spherical mirrors are presented. These formulae which are derived from the marginal ray fan equation can be used for designing laser cavities, spectrographs and adaptive optics retinal imaging systems. The use, range and validity of these formulae are limited by spherical aberration and coma for small and large angles respectively. This is discussed using examples from adaptive optics retinal imaging systems. The performance of the resulting optical designs are evaluated and compared against the configurations with minimal wavefront RMS, using the defocus-corrected wavefront RMS as a metric.

OCIS codes: (110.1080) Active or adaptive optics, (080.2468) First-order optics, (080.4035) Mirror system design, 220.1000 Aberration compensation, (330.4460) Ophthalmic optics and devices.

References

1. J. Liang, D. R. Williams, and D. T. Miller, "Supernormal vision and high-resolution retinal imaging through adaptive optics," J. Opt. Soc. Am. A **14**(11), 2884–2892 (1997), http://www.opticsinfobase.org/abstract.cfm?URI=josaa-14-11-2884.
2. J. Rha, R. S. Jonnal, K. E. Thorn, J. Qu, Y. Zhang, and D. T. Miller, "Adaptive optics flood-illumination camera for high speed retinal imaging," Opt. Express **14**(10), 4552–4569 (2006), http://www.opticsinfobase.org/abstract.cfm?URI=oe-14-10-4552.
3. B. Hermann, E. J. Fernández, A. Unterhuber, H. Sattmann, A. F. Fercher, W. Drexler, P. M. Prieto, and P. Artal, "Adaptive-optics ultrahigh-resolution optical coherence tomography," Opt. Lett. **29**(18), 2142–2144 (2004), http://www.opticsinfobase.org/ol/abstract.cfm?URI=ol-29-18-2142.
4. R. J. Zawadzki, S. M. Jones, S. S. Olivier, M. T. Zhao, B. A. Bower, J. A. Izatt, S. Choi, S. Laut, and J. S. Werner, "Adaptive-optics optical coherence tomography for high-resolution and high-speed 3D retinal in vivo imaging," Opt. Express **13**(21), 8532–8546 (2005), http://www.opticsinfobase.org/oe/abstract.cfm?URI=oe-13-21-8532.
5. E. J. Fernández, B. Povazay, B. Hermann, A. Unterhuber, H. Sattmann, P. M. Prieto, R. Leitgeb, P. Ahnelt, P. Artal, and W. Drexler, "Three-dimensional adaptive optics ultrahigh-resolution optical coherence tomography using a liquid crystal spatial light modulator," Vision Res. **45**(28), 3432–3444 (2005).
6. Y. Zhang, J. T. Rha, R. S. Jonnal, and D. T. Miller, "Adaptive optics parallel spectral domain optical coherence tomography for imaging the living retina," Opt. Express **13**(12), 4792–4811 (2005), http://www.opticsinfobase.org/oe/abstract.cfm?URI=oe-13-12-4792.
7. D. Merino, C. Dainty, A. Bradu, and A. G. Podoleanu, "Adaptive optics enhanced simultaneous en-face optical coherence tomography and scanning laser ophthalmoscopy," Opt. Express **14**(8), 3345–3353 (2006), http://www.opticsinfobase.org/abstract.cfm?URI=oe-14-8-3345.
8. C. E. Bigelow, N. V. Iftimia, R. D. Ferguson, T. E. Ustun, B. Bloom, and D. X. Hammer, "Compact multimodal adaptive-optics spectral-domain optical coherence tomography instrument for retinal imaging," J. Opt. Soc. Am. A **24**(5), 1327–1336 (2007), http://www.opticsinfobase.org/abstract.cfm?URI=josaa-24-5-1327.
9. A. Roorda, F. Romero-Borja, W. Donnelly Iii, H. Queener, T. J. Hebert, and M. C. W. Campbell, "Adaptive optics scanning laser ophthalmoscopy," Opt. Express **10**(9), 405–412 (2002), http://www.opticsinfobase.org/oe/abstract.cfm?URI=oe-10-9-405.
10. Y. Zhang, S. Poonja, and A. Roorda, "MEMS-based adaptive optics scanning laser ophthalmoscopy," Opt. Lett. **31**(9), 1268–1270 (2006), http://www.opticsinfobase.org/ol/abstract.cfm?URI=ol-31-9-1268.

#112822 - $15.00 USD Received 22 Jun 2009; revised 11 Sep 2009; accepted 12 Sep 2009; published 6 Oct 2009

11. D. X. Hammer, R. D. Ferguson, C. E. Bigelow, N. V. Iftimia, T. E. Ustun, and S. A. Burns, "Adaptive optics scanning laser ophthalmoscope for stabilized retinal imaging," Opt. Express **14**(8), 3354–3367 (2006), http://www.opticsinfobase.org/oe/abstract.cfm?URI=oe-14-8-3354.
12. D. C. Gray, W. Merigan, J. I. Wolfing, B. P. Gee, J. Porter, A. Dubra, T. H. Twietmeyer, K. Ahamd, R. Tumbar, F. Reinholz, and D. R. Williams, "In vivo fluorescence imaging of primate retinal ganglion cells and retinal pigment epithelial cells," Opt. Express **14**(16), 7144–7158 (2006), http://www.opticsinfobase.org/oe/abstract.cfm?URI=oe-14-16-7144.
13. S. A. Burns, R. Tumbar, A. E. Elsner, D. Ferguson, and D. X. Hammer, "Large-field-of-view, modular, stabilized, adaptive-optics-based scanning laser ophthalmoscope," J. Opt. Soc. Am. A **24**(5), 1313–1326 (2007), http://www.opticsinfobase.org/abstract.cfm?URI=josaa-24-5-1313.
14. R. H. Webb, and G. W. Hughes, "Scanning laser ophthalmoscope," IEEE Trans. Biomed. Eng. **BME-28**(7), 488–492 (1981).
15. R. H. Webb, G. W. Hughes, and F. C. Delori, "Confocal scanning laser ophthalmoscope," Appl. Opt. **26**(8), 1492–1499 (1987).
16. H. W. Kogelnik, E. P. Ippen, A. Dienes, and C. V. Shank, "Astigmatically compensated cavities for CW dye lasers," IEEE J. Quantum Electron. **8**(3), 373–379 (1972).
17. W. T. Foreman, "Lens Correction of Astigmatism in a Czerny-Turner Spectrograph," Appl. Opt. **7**(6), 1053–1059 (1968), http://www.opticsinfobase.org/ao/abstract.cfm?URI=ao-7-6-1053.
18. G. R. Rosendahl, "Contributions to the Optics of Mirror Systems and Gratings with Oblique Incidence. III. Some Applications," J. Opt. Soc. Am. **52**(4), 412–415 (1962), http://www.opticsinfobase.org/josa/abstract.cfm?URI=josa-52-4-412.
19. A. E. Conrady, *Applied Optics and Optical Design*, (Dover Publications Inc., New York, 1960), Chap XII, part 2.
20. D. Malacara, and Z. Malacara, *Handbook of Lens Design*, (Marcel Dekker Inc., New York. 2004), Chap. 5.
21. R. Kingslake, *Lens Design Fundamentals*, (Academic Press, San Diego, 1978), Chap 10.
22. D. A. Atchison, A. Bradley, L. N. Thibos, and G. Smith, "Useful variations of the Badal optometer," Optom. Vis. Sci. **72**(4), 279–284 (1995).
23. G. Smith, and D. A. Atchison, *The eye and visual optical instruments*, (Cambridge University Press, Cambridge, U.K., 1997), Chap. 30.

1. Introduction

The introduction of adaptive optics (AO) to ophthalmic imaging in recent years has led to the development of a new generation of high-resolution retinal imaging instruments. These include the AO fundus camera [1,2], the AO optical coherence tomograph (AO-OCT) [3–8] and the AO scanning laser ophthalmoscope (AOSLO) [7,9–13]. Refractive systems are not desirable for these applications given that the back reflections from the optical surfaces can be orders of magnitude brighter than the light scattered or emitted by the retina. For example, the light scattered from human cone photoreceptors in these instruments is 10^{-3}-10^{-4} times lower than the illumination, while the broadband anti-reflection coatings required for the typical broadband sources used in these instruments reflect as much as 10^{-2}. Broadband sources are essential for minimizing speckle and/or increasing axial resolution in all the scattered light imaging modalities. Current low-resolution clinical instruments do not suffer from such back reflection problems because they use different portions of the eye's pupil for illumination and light collection. AO retinal imaging instruments however, need to use the full pupil of the eye for both illumination and imaging in order to achieve maximum lateral and axial resolution. The pupil (aperture stop) of the human eye is defined by the iris, and the planes conjugate to it are referred to as "pupil planes." In order to minimize back reflections, most AO-equipped scanning ophthalmic instruments are at least partially built using off-axis spherical mirrors [1,4,7–13]. Spherical mirrors are preferred over aspheres, given their lower cost and ease of alignment.

Due to the off-axis arrangement, the major optical performance limitation of such systems is astigmatism. This is described by Webb *et al*. [14,15] when reporting the first confocal scanning laser ophthalmoscope, and later by Burns *et al.* [13]. In his work, Webb suggests an off-the-plane perpendicular folding of the optical setup to reduce the astigmatism present in the pupil plane which degrades the image quality in the retinal planes. Since then, the design of AO retinal imaging instruments has been dominated by efforts to improve the retinal image quality, while largely ignoring the aberrations in retinal conjugate planes. Aberrations in retinal planes degrade the image quality at the pupil planes, where the wavefront sensor and corrector(s) are placed. The poor image quality at the pupil planes affects the quality of the AO correction. In the best case scenario, this results in a reduced temporal bandwidth of the

#112822 - $15.00 USD Received 22 Jun 2009; revised 11 Sep 2009; accepted 12 Sep 2009; published 6 Oct 2009

closed-loop AO performance. In the worst case scenario, the higher spatial frequency aberrations will be attenuated to the extent that they cannot be sensed, and therefore, not corrected.

Even though the motivation for this work is improving the performance of AO ophthalmic instruments, other reflective optical systems based on off-axis spherical mirrors, such as spectrographs and laser cavities, can benefit from the astigmatism compensation presented here. In the past, astigmatism compensation in such systems has been performed by adding glass plates [16], lenses [17] or additional convex mirrors [18] among other methods.

In this work, expressions for designing minimal astigmatism optical systems based on pairs of off-axis reflective 4f telescopes using spherical mirrors are derived. In what follows we refer to image planes (retina conjugates) as "infinite conjugates" and the pupil planes as a particular case of "finite conjugates." First, the marginal ray fan equation, the geometry of the off-axis reflective telescope and the astigmatism equations will be introduced. Then the particular cases of small angles of incidence with an object point at the front focal point of the telescope (pupil) and at infinity (retina) will be evaluated. A discussion of the sensitivity of the astigmatism-corrected designs to focus shifts and to Badal shifts (i.e. mirror separation change) will follow. Finally, examples illustrating the range of validity of the derived formulae, and the optical performance of the corresponding designs will be presented.

2. Theory

2.1 General marginal ray fan equation

In the paraxial theory of on-axis rotationally symmetric optical elements in a medium, rays emerging from a point object converge onto an image point. The first-order image formation of such optical components can be described by the Gaussian equation for a thin element that takes the well-known form

$$\frac{1}{s}+\frac{1}{s'}=\frac{1}{f}, \tag{1}$$

where s and s' are object and image distances from the optical element respectively, and f is the focal length of the optical element. For off-axis objects, the marginal rays converge at different points along the principal ray, depending on the orientation θ of the plane defined by the principal ray and the corresponding marginal ray. To first order approximation, the distances along the principal ray between the optical element and the marginal images under the thin lens approximation are given by the general marginal ray fan equation [19], which for spherical mirrors takes the form

$$\frac{1}{s}+\frac{1}{s_\theta'}=\frac{2\cos I}{r\,(1-\cos^2\theta\sin^2 I)}, \tag{2}$$

where I is the angle of incidence of the principal ray onto the mirror, and r is the radius of curvature of the mirror. For the special cases $\theta=\pi/2$ and $\theta=0$, one recovers the more familiar Coddington equations [20,21] that give the position of the sagittal and tangential images respectively,

$$\frac{1}{s_s}+\frac{1}{s_s'}=\frac{2\cos I}{r}, \tag{3}$$

$$\frac{1}{s_t}+\frac{1}{s_t'}=\frac{2}{r\cos I}. \tag{4}$$

As will be shown later, it is sometimes convenient to rewrite the marginal ray fan equation in terms of vergences $\phi=1/s,$ rather than distances,

#112822 - $15.00 USD Received 22 Jun 2009; revised 11 Sep 2009; accepted 12 Sep 2009; published 6 Oct 2009

$$\phi + \phi_\theta' = \frac{2\cos I}{r\,(1-\cos^2\theta \sin^2 I)}. \tag{5}$$

For an off axis spherical mirror and an object point at infinity, the focal length as a function of angle of incidence can be defined as the average of the sagittal and tangential distances along the principal ray,

$$f(I) = \frac{r\left[3+\cos(2I)\right]}{8\cos I}. \tag{6}$$

The position of the average mirror focus defined in this way, corresponds to the circle of least confusion, which for angles of incidence smaller than 30°, can be approximated by its on-axis value (with less than 1% error)

$$f(I) \approx \frac{r}{2}. \tag{7}$$

2.2 Minimization of astigmatism in afocal telescopes

To date, most reflective AO ophthalmic systems consist of a number of off-axis afocal telescopes that relay the pupil of the eye onto the wavefront sensor, wavefront corrector(s) and scanning devices. When these telescopes are formed by pairs of spherical mirrors, they are fully described by the five parameters shown in Fig. 1: the angles of incidence I_1 and I_2 of the principal ray onto the mirrors m_1 and m_2; the mirror radii of curvature r_1 and r_2, and the angle θ between the planes defined by the incident and reflected principal rays. In what follows, unless otherwise stated, it is assumed that the separation between mirrors along the principal ray is the sum of the on-axis mirror focal lengths, which is $d = (r_1 + r_2)/2$, as it is usually implied when referring to afocal telescopes. The dominant aberration in these telescopes is astigmatism. Astigmatism occurs when ray fans passing through different planes containing the principal ray focus at different points along the principal ray. By an appropriate selection of the telescope parameters, astigmatism can be eliminated along the principal ray for one or at most two image points, as is shown next.

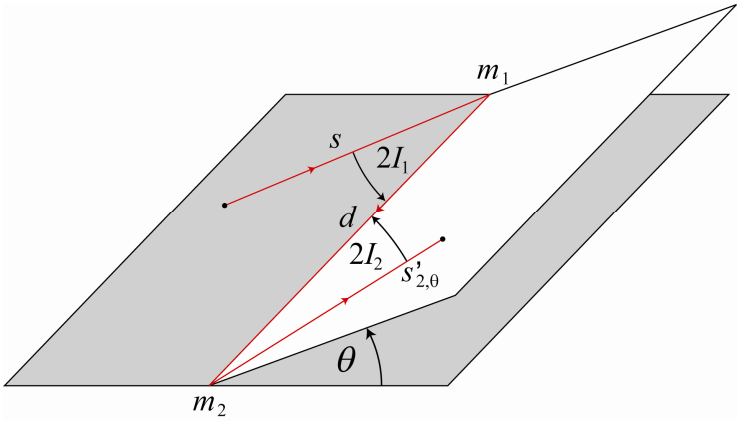

Fig. 1. Geometry of an off-axis reflective afocal telescope: I_1 and I_2 are the angles of incidence of the principal ray (in red) onto the mirrors m_1 and m_2 respectively, and the angle θ between the incidence planes. The object is a distance s from the first mirror, and the image formed by the second mirror is a distance $s'_{2,\theta}$ from it.

Consider the sagittal and tangential images formed by the telescope from a point source a distance s from the first telescope mirror. If these marginal images coincide, then the images

#112822 - $15.00 USD Received 22 Jun 2009; revised 11 Sep 2009; accepted 12 Sep 2009; published 6 Oct 2009

from all other ray fans will also coincide, provided that the only aberration present is astigmatism. Thus, by bringing these images together, the relationship between the telescope parameters that eliminates astigmatism for the particular point can be found. By applying Eq. (2) successively to each mirror, one gets that the separation between the sagittal and tangential images is given by

$$\Delta_s = \frac{r_2\left(\sin^2\theta\sin^2 I_2 - 1\right)\left[\dfrac{s\,r_1}{r_1 - 2s\cos I_1} + d\right]}{r_1\cos I_2\left(d + \dfrac{sr_1}{r_1 - 2s\cos I_1}\right) + r_2\left(\sin^2\theta\sin^2 I_2 - 1\right)} - \frac{r_2\left(\cos^2\theta\sin^2 I_2 - 1\right)\left[\dfrac{s\,r_1\cos I_1}{r_1\cos I_1 - 2s} + d\right]}{2\cos I_2\left(d + \dfrac{s\,r_1\cos I_1}{r_1\cos I_1 - 2s}\right) + r_2\left(\cos^2\theta\sin^2 I_2 - 1\right)}. \quad (8)$$

For small angles of incidence (I_1 and I_2), and $d = (r_1 + r_2)/2$, Eq. (8) can be expressed in terms of the telescope magnification $M = r_2 / r_1$ as

$$\Delta_s \approx -\frac{M\,r_1\cos(2\theta)}{2}\left(1 + M - \frac{2Ms}{r_1}\right)^2 I_2^{\,2} - \frac{2s^2M^2}{r_1} I_1^{\,2}. \quad (9)$$

The corresponding astigmatism equations in terms of vergence rather than object distance are

$$\Delta_\phi = \frac{r_1\phi - 2\cos I_1}{d\left(r_1\phi - 2\cos I_1\right) + r_1} + \frac{2 - \phi\, r_1\cos I_1}{(1 + \phi\, d)\cos I_1 r_1 - 2d} + \frac{2\cos I_2}{r_2(\cos^2\theta\sin^2 I_2 - 1)} + \frac{2\cos I_2}{r_2\left(1 - r_2\sin^2\theta\sin^2 I_2\right)}, \quad (10)$$

and,

$$\Delta_\phi \approx \frac{2\cos(2\theta)}{r_2} I_2^{\,2} + \frac{8}{r_1\left[r_1\phi\left(1 + M\right) - 2M\right]^2} I_1^2. \quad (11)$$

2.2.1 Finite conjugate (s = r_1/2)

Pupil planes in AO scanning ophthalmic instruments are typically placed one focal length in front of the first telescope mirror, (i.e. r_1/2 according to Eq. (7)). The astigmatism in these planes is described by Eqs. (8) and (9) with the geometry depicted in Fig. 2. When substituting s with r_1/2 in Eq. (9), the following condition for astigmatism cancellation is obtained,

$$I_2 \approx \sqrt{-\frac{M}{\cos(2\theta)}}\, I_1. \quad (12)$$

#112822 - $15.00 USD Received 22 Jun 2009; revised 11 Sep 2009; accepted 12 Sep 2009; published 6 Oct 2009

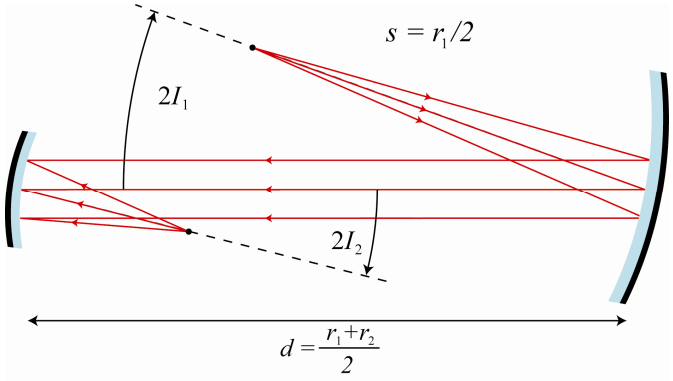

Fig. 2. Notation used to describe an afocal telescope formed by a pair of off-axis spherical mirrors in the finite conjugate case, with s = r1/2. This particular configuration corresponds to θ = 0.

This condition can only be met if $\pi/4 < |\theta| < 3\pi/4$, which is reasonable, given that the second mirror must introduce less astigmatism on the incidence plane of the first mirror than on the perpendicular plane. The particular case $\theta = \pi/2$ produces the most compact optical setup (i.e. the one with the smallest I_2), therefore minimizing other field-dependent aberrations.

Meeting the condition in Eq. (12) cancels the astigmatism for the object point at $s = r_1/2$ along the principal ray, and minimizes the overall astigmatism for other points within a field of view centered on the object point. To illustrate this, consider the astigmatism corresponding to an arbitrary point in the same plane and near the point with null astigmatism. The angles of incidence of the principal ray corresponding to this new point can be expressed as $I_1 + \varepsilon_1$, with $\varepsilon_1 < I_1$, and $I_2 + \varepsilon_2$, with $\varepsilon_2 < I_2$. Substituting in Eq. (9) and imposing the condition in Eq. (12) yields

$$\Delta_s \propto r_1 M^2 I_1 \varepsilon_1 . \tag{13}$$

This result shows that the astigmatism over the field of view is proportional to the angle of incidence I_1, and therefore, whenever possible, small angles of incidence should be used. Similarly, low magnification telescopes and short focal length mirrors will also result in low astigmatism over the field of view. Finally, the linear dependence in ε_1 indicates that the astigmatism will be minimal when the condition in Eq. (12) is met for the point at the center of the field of view.

2.2.2 Infinite conjugates

The second set of relevant optical planes in ophthalmic instruments with AO is the image planes, which are conjugated to the retina. Because the light exiting the relaxed emmetropic eye is nearly collimated, it is more convenient to work with vergences rather than distances. Therefore, with the geometry depicted in Fig. 3 and substituting $\phi = 0$ in Eq. (11), the condition for minimizing astigmatism in image planes becomes

$$I_2 \approx \sqrt{-\frac{1}{M\cos(2\theta)}}\, I_1 . \tag{14}$$

#112822 - $15.00 USD Received 22 Jun 2009; revised 11 Sep 2009; accepted 12 Sep 2009; published 6 Oct 2009

Similar to the finite conjugates case, this condition can only be met if $\pi/4 < |\theta| < 3\pi/4$. Note that while astigmatism is only cancelled for a point at infinity along the principal ray, the overall astigmatism for any point within a symmetric field of view is also minimized as before. Following the same steps that led to relation (13), using Eqs. (11) and (14) yields

$$\Delta_\phi \propto \frac{4I_1}{M}\left(\frac{\varepsilon_2}{r_2}+\frac{\varepsilon_1}{r_1}\right). \tag{15}$$

As in the finite conjugate case studied above, small angles of incidence will result in configurations with lower astigmatism over the field of view. Contrary to the previous case however, high magnification and long focal lengths will reduce the astigmatism across the field of view. This means that in order to have a single telescope with low astigmatism in both pupil and retinal planes, the angles of incidence should be kept to a minimum.

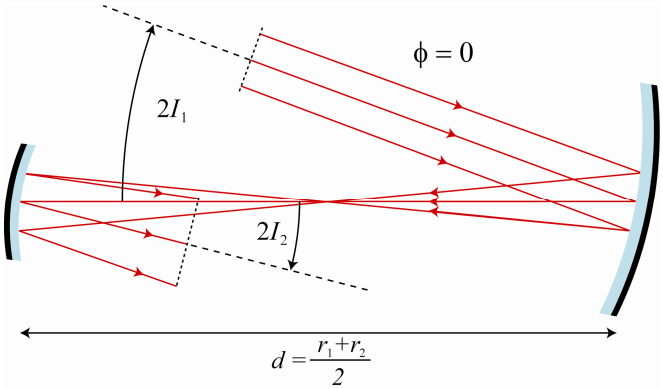

Fig. 3. Notation used to describe an afocal telescope formed by a pair of off-axis spherical mirrors in the infinite conjugates case. This particular arrangement corresponds to the case $\theta = 0$.

2.3 Simultaneous minimization of astigmatism in pupil and image planes in pairs of afocal telescopes

Typically, optical elements such as scanners, wavefront correctors, wavefront sensors and trial lenses are placed in the pupil planes of retinal imaging instruments equipped with AO. As mentioned earlier, in order to take full advantage of the AO correction, astigmatism needs to be corrected so that image quality is good in all pupil planes. The astigmatism affecting retinal planes however, only needs to be corrected at the ends of the optical setup, that is, at the eye and the science detector(s). This dictates that all the telescopes in such systems should meet the condition in Eq. (12) to compensate for astigmatism in the pupil planes. By comparing Eqs. (12) and (14), it is clear that astigmatism can only be minimized simultaneously in both pupil and image planes for telescopes with unit magnification. However, when selecting the second angle of incidence in terms of the first one as prescribed by Eq. (12), a degree of freedom in the selection of the first angle of incidence remains. Thus, by combining a pair of pupil-corrected telescopes, the first angle of each of the telescopes can be selected to minimize astigmatism in the exit image plane, while preserving minimal astigmatism in all the pupil planes.

For example, consider a pair of pupil-corrected (i.e. minimal astigmatism) telescopes in series,

$$I_2 \approx \sqrt{-\frac{M_{12}}{\cos(2\theta_{12})}}\, I_1,\ I_4 \approx \sqrt{-\frac{M_{34}}{\cos(2\theta_{34})}}\, I_3. \tag{16}$$

#112822 - $15.00 USD Received 22 Jun 2009; revised 11 Sep 2009; accepted 12 Sep 2009; published 6 Oct 2009

By calculating the vergence difference between the marginal ray fans from an object at infinity after the reflections on all four mirrors, the condition for minimizing astigmatism in the small angles regime can be obtained,

$$I_3 = \frac{1}{M_{12}} \sqrt{\frac{-r_3\left(1-{M_{12}}^2\right)\cos(2\theta_{34})}{r_1\left\{M_{34}^2 \sin\left[2\left(\theta_{12}+\theta_{23}\right)\right]\sin\left(2\theta_{34}\right)+\left(1-M_{34}^2\right)\cos\left[2\left(\theta_{12}+\theta_{23}\right)\right]\cos\left(2\theta_{34}\right)\right\}}}\, I_1 . \quad (17)$$

As in the previous two sections, this condition cancels the astigmatism for the point along the optical axis and minimizes the average astigmatism over the field of view. By considering the astigmatism-compensated configurations with smaller angles, i.e. $\left|\theta_{12}\right| = \left|\theta_{34}\right| = \pi/2$, and $\left|\theta_{23}\right| = 0, \pi/2, \pi$, other field-dependent aberrations will also be reduced. For these configurations, Eq. (17) becomes

$$I_3 \approx \frac{1}{M_{12}} \sqrt{\pm\frac{r_3}{r_1}\left(\frac{1-{M_{12}}^2}{1-{M_{34}}^2}\right)}\, I_1 . \quad (18)$$

The sign inside the radical depends on whether $\left|\theta_{23}\right| = 0, \pi$ or $\pi/2$. This gives rise to two families of telescope configurations with minimal astigmatism: one in which $M_{12} > 1$ and $M_{34} < 1$ ($\left|\theta_{23}\right| = \pi/2$), and one in which $M_{12} < 1$ and $M_{34} < 1$ ($\left|\theta_{23}\right| = 0, \pi$). An example to illustrate this point will be discussed in the examples section below.

The same steps could be used to obtain an astigmatism cancellation condition for a three-telescope system. With six mirrors instead of four, there would be an infinite number of solutions, instead of just eight as in Eq. (18).

2.4 Impact of focus shift on astigmatism minimization

By calculating the astigmatism introduced by a focus shift in off-axis afocal reflective telescopes, the robustness to beam collimation and to axial alignment can be studied. Indeed, it is sometimes desirable to shift the focus of the retinal planes to image different structures and/or compensate for chromatic aberration when imaging using multiple wavelengths. The expansion of Eqs. (8) and (10) for small angles in the presence of a small defocus, that is $s = r_1/2 + \varepsilon_s$, with $2\left|\varepsilon_s\right|/r_1 << 1$, and $\phi = \varepsilon_\phi$, with $r_1\left|\varepsilon_\phi\right|/2 << 1$ respectively, give

$$\Delta_s \approx -\frac{r_1 M\cos(2\theta)}{2} {I_2}^2 - \frac{r_1 M^2}{2} {I_1}^2 + \left[2M^2\cos(2\theta){I_2}^2 - 2M^2{I_1}^2\right]\varepsilon_s \quad (19)$$

and

$$\Delta_\phi \approx \frac{2\cos(2\theta)}{r_1 M} {I_2}^2 + \frac{2}{r_1 M^2} I_1^2 + 2\left(\frac{1}{M^3}+\frac{1}{M^2}\right) I_1^2 \varepsilon_\phi . \quad (20)$$

These equations indicate that in the general case, the astigmatism introduced by small focus shifts corresponds to third order terms (i.e. $I_1^2\varepsilon_s$, $I_2^2\varepsilon_s$ and $I_1^2\varepsilon_\phi$) and is therefore negligible compared to the dominant second order terms(I_1^2, I_2^2). However, for pupil or image plane astigmatism-corrected telescopes, the astigmatism introduced by the focus shift is the dominant term,

$$\Delta_s \approx -2M^2\left(1+M\right) I_1^2 \varepsilon_s , \quad (21)$$

$$\Delta_\phi \approx 2\frac{1}{M^2}\left(\frac{1}{M}+1\right) I_1^2 \varepsilon_\phi . \quad (22)$$

#112822 - $15.00 USD Received 22 Jun 2009; revised 11 Sep 2009; accepted 12 Sep 2009; published 6 Oct 2009

It is clear then that reducing the angles of incidence increases the tolerance to focus shifts simultaneously in both sets of planes and independently of the telescopes' magnification.

Applying the same idea to a pair of afocal telescopes that simultaneously meet conditions (16) and (18), yields that the astigmatism in the image plane as a result of a small focus shift is given by

$$\begin{aligned}\Delta_\phi = &\left\{ r_3^2 \left[r_2 M_{12} + r_3 \left(M_{12} - 1 \right) \right] \cos\left[2\left(\theta_{12} + \theta_{23} \right) \right] \cos\left(2\theta_{34} \right) \right. \\ &\left. - r_3^2 r_4 \left(1 - M_{12} \right) \cos\left[2\left(\theta_{12} + \theta_{23} + \theta_{34} \right) \right] - r_2 r_4^2 M_{12} \cos\left[2\left(\theta_{12} + \theta_{23} + \theta_{34} \right) \right] \right\} \\ &\times \frac{2\left(1 + M_{12} \right)}{r_2 M_{12}^3 M_{34}^2 \left\{ r_3^2 \cos\left[2\left(\theta_{12} + \theta_{23} \right) \right] \cos\left(2\theta_{34} \right) - r_4^2 \cos\left[2\left(\theta_{12} + \theta_{23} + \theta_{34} \right) \right] \right\}} \, I_1^2 \, \varepsilon_\phi ,\end{aligned} \tag{23}$$

with the defocus term being a third order term, as before. As in the case of a single telescope, the impact of the defocus shift can be reduced by selecting small angles of incidence.

2.5 The off-axis Badal optometer

Many ophthalmic imaging instruments use the Badal optometer [22,23], to either partially or completely compensate for the refractive error of the eye. In these instruments, a positive lens (the Badal lens) is kept a focal length away from the eye, while its distance to the instrument is adjusted until the retinal image is in focus (Badal shift). This can also be achieved using a concave mirror. In the off-axis afocal telescopes discussed in this work, a Badal shift would introduce an undesired astigmatism component in the retinal plane. This astigmatism would be negligible in comparison to the defocus being compensated for, provided the angles of incidence on the telescope mirrors are small, as it is shown next.

In an off axis pupil-corrected afocal telescope, changing the mirror separation $d = (r_1 + r_2)/2$ by a small amount ($|\varepsilon_d| << (r_1 + r_2)/2$) introduces astigmatism in the pupil plane. This astigmatism can be calculated by substituting in Eq. (8) and performing a polynomial expansion retaining only the lower order terms,

$$\Delta_d \approx \frac{1 - M}{3 r_1} I_1^4 + \frac{\left(1 + M \right)\left(211 + 59M \right)}{180 r_1} I_1^6 + \frac{3 + 2M}{r_1^2} I_1^6 \varepsilon_d . \tag{24}$$

This expression indicates that for small angles of incidence and to 6th order, the pupil astigmatism is independent of the Badal adjustment.

3. Examples

In this section we evaluate the performance of three systems. The first and second are single telescopes corrected for astigmatism in the pupil and image planes respectively. The third is a pair of telescopes with astigmatism corrected in the entrance and exit image planes, as well as all three pupil planes. For comparison, the angles predicted by the marginal ray fan Eqs. (8) and (10), their linear approximations, that is Eqs. (12), (14) and (18) and, the optimal angles determined by minimizing the wavefront RMS are presented. In all examples, the wavefront RMS was calculated using the ray tracing software from Zemax Development Corporation (Bellevue, Washington, USA) after correcting for defocus. Optimization in Zemax was performed by allowing the program to vary only the second angle of incidence when considering a single telescope. When considering two telescopes in sequence, only the third angle of incidence was varied, with the second and fourth angles calculated using Eqs. (16).

3.1 Single off-axis afocal telescope finite conjugate corrected ($s = r_1/2$)

In order to illustrate the dependence on telescope magnification and folding angle θ, three telescopes are evaluated. The first is a 2:1 telescope with a 90° folding angle. The second and

#112822 - $15.00 USD Received 22 Jun 2009; revised 11 Sep 2009; accepted 12 Sep 2009; published 6 Oct 2009

third are 3:1 and 2:1 telescopes with 90° and 80° folding angles respectively. The results are presented in Fig. 4.

The plots on the top row compare the results of solving Eq. (8) exactly with its linear approximation given by Eq. (12). These results are also compared to the optimal angle which minimizes the wavefront RMS as calculated by Zemax. The plots show that for θ = 90°, the angles predicted by the marginal ray fan equation (Coddington) and its linear approximation minimize the wavefront RMS for angles of incidence ≥ 1°. The prediction of the optimal angle is not as good for the θ = 80° configuration due to the presence of coma. The plots on the second row show how the axial separation of the image point from the second mirror decreases with increasing angles of incidence. This is also the case for magnifications greater than one. The plots on the bottom row show the corresponding wavefront RMS values for all the configurations, including the planar case ($\theta = 0^{\circ}$) for reference. The most outstanding feature in all three plots is that by folding the telescope off the plane, the wavefront RMS decreases by an order of magnitude. Also, the Coddington solution and its linear approximation are virtually identical to that of the optimal configuration. This means that the linear approximation model in Eq. (12) is acceptable for all practical purposes in the 1 to 15° range. For angles less than 1°, the predicted angles are far from optimal because of the presence of spherical aberration. Finally, it should be noted that the 90° configuration produces the smallest second angle of incidence, hence minimizing other aberrations. This is illustrated by comparing the first and third plots of the bottom row.

3.2 Single off-axis afocal telescope infinite conjugate corrected

The performance of the three previously described telescopes is evaluated with an object point placed at infinity. The results are displayed in Fig. 5.

The plots on the top row compare the results of solving Eq. (10) exactly, with its linear approximation given by Eq. (14). These results are also compared to the optimal angle which minimizes the wavefront RMS. For the θ = 90° configurations, the angles predicted by the Coddington equation and its linear approximation minimize the wavefront RMS over a range of 1 to 5°. This is significantly limited compared to the results of the previous section. The estimation of the second angle of incidence is poorer for the θ = 80° configuration due to the presence of coma. The plots on the second row show that the vergence of the beam reflected off the second mirror becomes more negative with increasing angles of incidence. The same effect is observed for magnifications greater than one. The plots on the bottom row show the corresponding wavefront RMS values for all the configurations, including the planar case for reference. The exact Coddington solution and its linear approximation perform better than the planar configuration, but the optimal configuration results in a more significant improvement for angles larger than 5°. This indicates that the linear approximation to the Coddington solution can be used as a starting point for the optimization software, which has to vary only two parameters to find the best solution. These parameters are the angle of incidence of the principal ray onto the second mirror and the vergence of the beam reflected by the second mirror. As in the previous section, spherical aberration dominates when angles of incidence are less than 1°. When angles of incidence are greater than 1°, the limiting aberration after astigmatism correction is coma. Coma is also the aberration that limits the range of validity of the linear approximation in Eq. (14). It should also be noted that the 90° configuration performs better than the 80° which is consistent with the results from the previous section.

3.3 Off-axis afocal telescopes pair finite and infinite conjugate corrected

The following example illustrates how to simultaneously correct astigmatism in both pupil and exit image planes by taking advantage of Eq. (18). The same reasoning could be applied to the more general Eq. (17), but for simplicity only the most compact designs (which also have the lowest wavefront RMS) will be discussed. The optical setup evaluated consists of a pair of reflective off-axis afocal telescopes in series, with the following spherical mirror radii of curvature in order: 1000, 500, 333 and 1000mm. Each of the two telescopes is pupil-

#112822 - $15.00 USD Received 22 Jun 2009; revised 11 Sep 2009; accepted 12 Sep 2009; published 6 Oct 2009

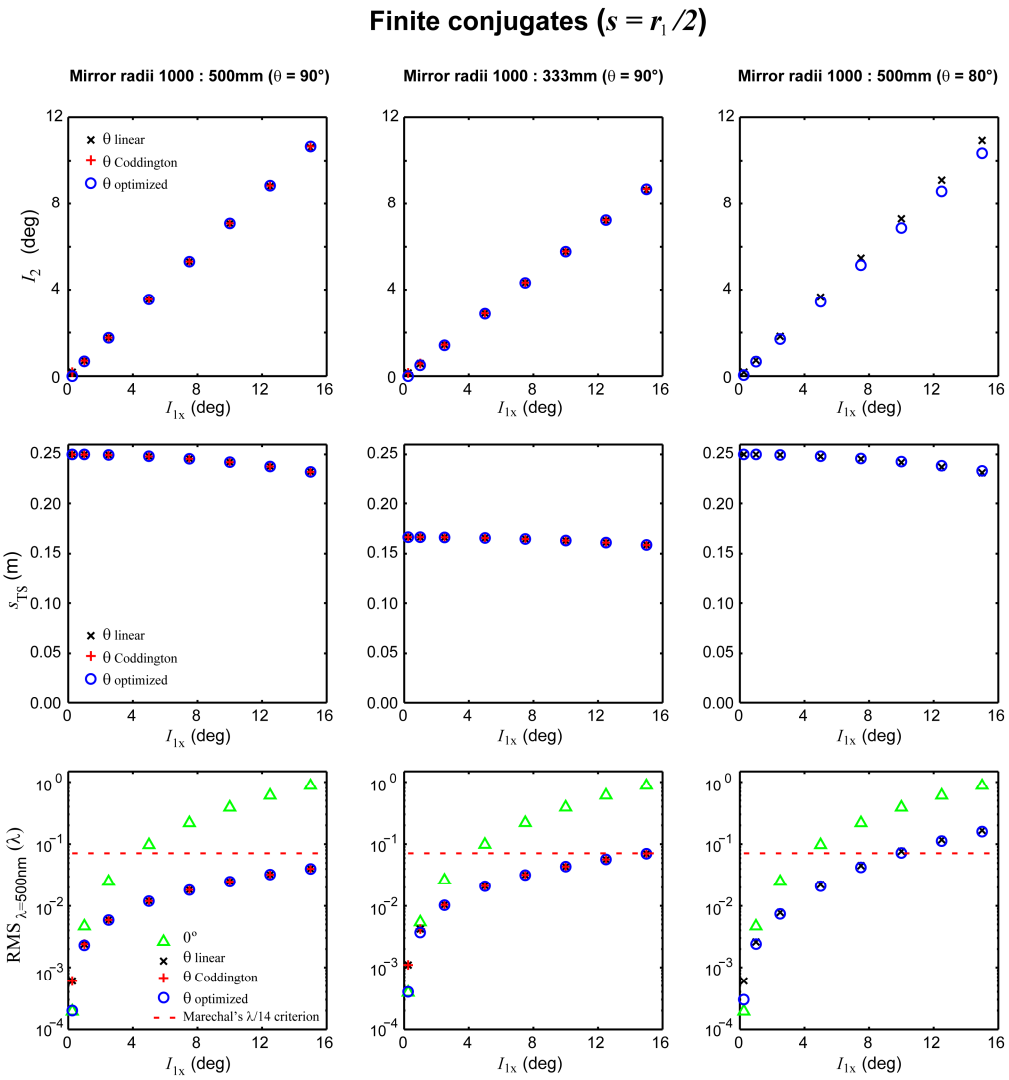

Fig. 4. Each column describes a different off-axis reflective afocal (4f) telescope, with the parameters indicated at the top. The object point is at the front focal point of the first mirror (Fig. 2). The top row shows the angle of incidence of the principal ray onto the second mirror as a function of the angle of incidence onto the first mirror. The second row shows the distance between the second mirror and the image point as a function of the first angle of incidence for the same configurations. The bottom row shows the wavefront RMS values for the (defocus-corrected) corresponding configurations. The RMS of the planar (θ = 0°) configuration is also plotted for comparison. The red dashed lines indicate Marechal's diffraction limit.

corrected using Eq. (16). Retinal astigmatism is corrected by either using the linear approximation in Eq. (16), or by optimization with the absolute values of θ_{12}, θ_{23} and θ_{34} being 90°. The separation between the two telescopes accounted for the focus shift shown in the middle row of Fig. 6.

As mentioned earlier, Eq. (18) has two families of solutions depending on the sign within the radical. The magnifications dictate which of the two families of solutions should be used. Each solution family is formed by four different configurations, given by the signs of θ_{23} and θ_{34}. The geometries of all 8 folding solutions are sketched in Table 1 below, and only the family of solutions that correspond to $|\theta_{23}| = \pi/2$ are plotted in Fig. 6.

#112822 - $15.00 USD Received 22 Jun 2009; revised 11 Sep 2009; accepted 12 Sep 2009; published 6 Oct 2009

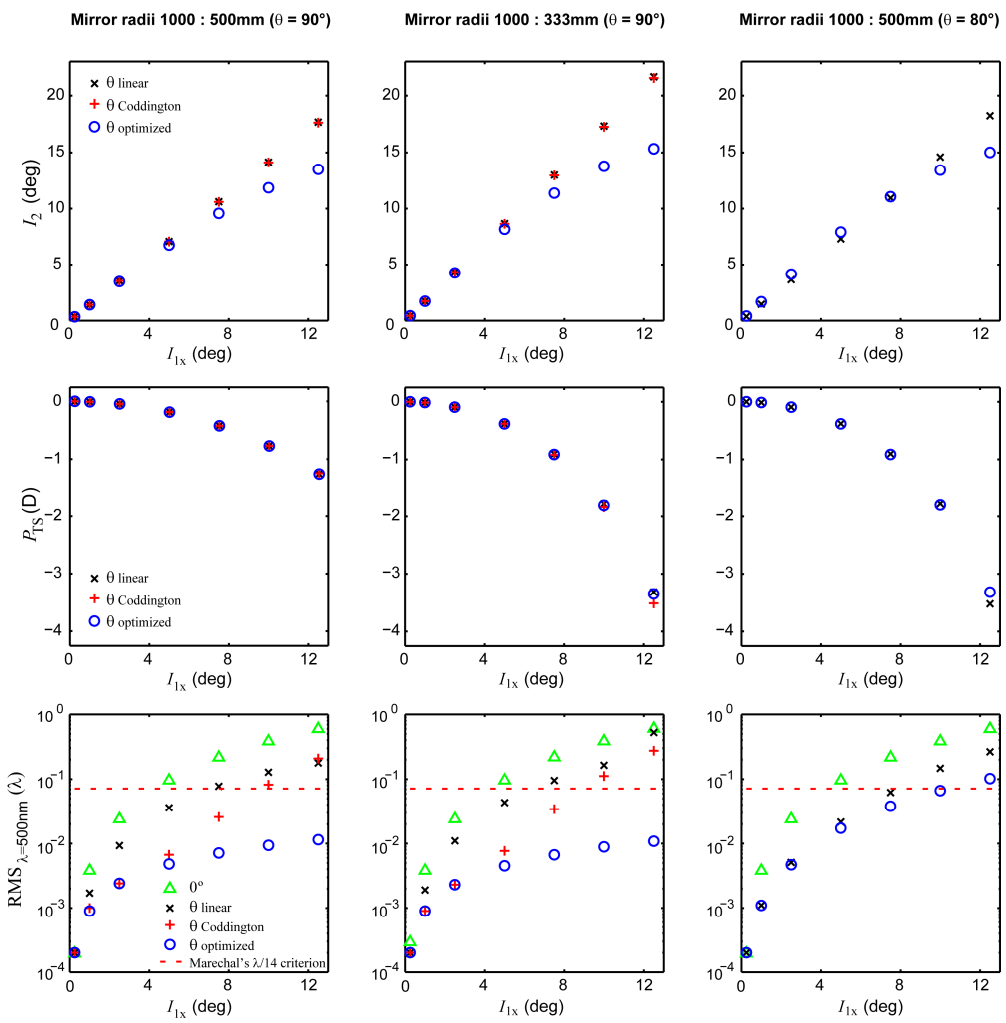

Fig. 5. Each column describes a different off-axis reflective afocal (4f) telescope, with the parameters indicated at the top. The object point is at the front focal point of the first mirror (see Fig. 3). The top row shows the angle of incidence of the principal ray onto the second mirror as a function of the angle of incidence onto the first mirror. The second row shows the power (vergence) between the second mirror and the image point in diopters (D) as a function of the first angle of incidence for the same configurations. The bottom row shows the wavefront RMS values for the (defocus-corrected) corresponding configurations. The RMS of the planar (θ = 0°) configuration is also plotted for comparison. The red dashed lines indicate Marechal's diffraction limit.

Astigmatism is minimized in all four configurations evaluated, but the impact of other aberrations (mostly coma) is different for each. This is shown by the four RMS values on the left side of the table. The plots in Fig. 6 show all four optimal configurations but only one solution of the linear approximation. This was done in order to maintain the readability of the plots. The first plot in Fig. 6 shows the angles calculated using Eq. (18) and the optimal angles for each of the four configurations sketched on the left side of Table 1. The linear approximation correctly predicts the optimal angles in the 1° to 5° range. The second plot shows the vergence of the beam reflected off the fourth mirror for all configurations. Similar to the single telescope case, the vergence becomes more negative with increasing angles of incidence. The third plot shows the corresponding wavefront RMS values for all the

#112822 - $15.00 USD Received 22 Jun 2009; revised 11 Sep 2009; accepted 12 Sep 2009; published 6 Oct 2009

Table 1. Wavefront RMS of the most compact configurations of two different pairs of off-axis telescopes with minimal aberrations, for $I_1 = 5°$. The numbers on the top row are the mirror radii of curvature in mm. The entrance beam diameter considered was 8mm and λ = 500nm.

	cos $(2\theta_3) = -1$ 1000: 500: 333: 1000				cos $(2\theta_3) = 1$ 500: 1000: 333: 1000			
θ_3, θ_4 Folding geometry	π/2, π/2	-π/2, π/2	π/2, -π/2	-π/2, -π/2	π, -π/2	0, -π/2	π, π/2	0, π/2
RMS (λ)	0.0064	0.0078	0.0089	0.0099	0.1502	0.1531	0.1638	0.1693

configurations at the image planes. The planar case is provided as a reference. The RMS for all non-planar configurations is significantly lower than for the planar design. The optical performance of the linear approximation is close to optimal in the 1° to 5° range. As in the previous cases, for angles less than 1°, the predicted angles are not optimal, due to spherical aberration.

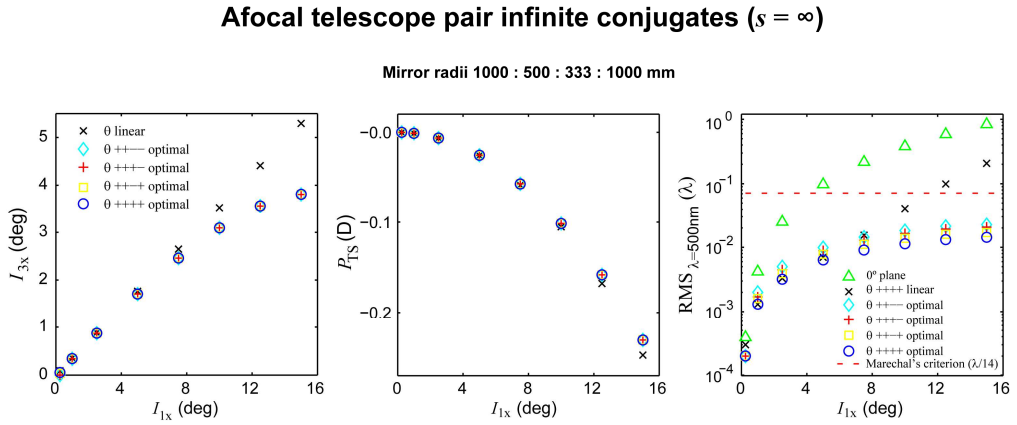

Fig. 6. Data from a pair of off-axis reflective afocal (4f) telescopes, with astigmatism simultaneously corrected in pupil and image planes. The left plot shows the angle of incidence of the principal ray onto the second mirror as a function of the angle of incidence onto the first mirror, for the linear approximation, and the four different optimal configurations sketched on the left side of Table 1. The middle plot shows the distance between the second mirror and the image point as a function of the angle of incidence. The plot on the right shows the wavefront RMS values for the (defocus-corrected) corresponding configurations. The RMS of the planar (θ = 0°) configuration is also plotted for comparison. The red dashed line in the last plot indicates Marechal's diffraction limit.

4. Conclusion

Expressions for minimal astigmatism in pupil and image planes applicable to off-axis reflective afocal telescopes were derived using the marginal ray fan equation. Three simple formulae, Eqs. (12), (14) and (18) for the small angle approximation were obtained and evaluated in different examples. The first two examples illustrate that by adequate off-plane folding, astigmatism can be corrected in the pupil or image planes of these telescopes. The third example shows that for a pair of reflective afocal telescopes, one could correct for astigmatism simultaneously in all the pupil planes and in the exit image plane. The formulae for a telescope pair could be directly applied to a system formed by any number of telescope pairs. The extension to a system with an odd number of telescopes has been discussed.

#112822 - $15.00 USD Received 22 Jun 2009; revised 11 Sep 2009; accepted 12 Sep 2009; published 6 Oct 2009

The obtained wavefront RMS plots show that the off-plane telescope configurations based on the conditions in Eqs. (12), (14) and (18), can perform an order of magnitude better than the corresponding planar configurations. It was also found that the 90° folding configuration always results in the lowest wavefront RMS, and in the particular cases presented here, below the diffraction limit.

It was also shown that reducing the angles of incidence on the studied reflective telescopes has multiple benefits. First, the astigmatism over the whole field of view is minimized. Second, other angle-dependent aberrations are also reduced. Finally, the system is more tolerant to axial misalignment and less sensitive (in terms of astigmatism) to Badal optometer-like shifts.

Even though the formulae presented were derived with AO ophthalmoscopy in mind, astigmatism minimization is desirable in other off-axis optical systems, such as spectrographs and laser cavities. To obtain these conditions, one simply has to calculate the difference between the sagittal and tangential images for the desired conjugate and number of mirrors, and solve for $\Delta_s = 0$.

Acknowledgements

The authors want to acknowledge the support of the Consejo Nacional de Ciencia y Tecnología de México (CONACyT), project No. 78812 and the scholar grant No. 170266. Alfredo Dubra-Suarez, Ph.D., holds a Career Award at the Scientific Interface from the Burroughs Welcome Fund. This research was also supported by the National Institute for Health, Bethesda, Maryland (NIH EY014375, NIH EY01319), Bausch and Lomb, Research to Prevent Blindness, the National Science Foundation, through the Center for Adaptive Optics, managed by the University of California at Santa Cruz (cooperative agreement no.: AST-9876783). We would like to thanks the reviewers and Yusufu Sulai for invaluable comments that have greatly improved the manuscript.

#112822 - $15.00 USD Received 22 Jun 2009; revised 11 Sep 2009; accepted 12 Sep 2009; published 6 Oct 2009